

Cloud cover and its impact on Brazil's deforestation satellite monitoring program

Sales, Vilane G.; Strobl, Eric; Elliott, Robert J.R.

DOI:

[10.1016/j.apgeog.2022.102651](https://doi.org/10.1016/j.apgeog.2022.102651)

License:

Creative Commons: Attribution (CC BY)

Document Version

Publisher's PDF, also known as Version of record

Citation for published version (Harvard):

Sales, VG, Strobl, E & Elliott, RJR 2022, 'Cloud cover and its impact on Brazil's deforestation satellite monitoring program: evidence from the cerrado biome of the Brazilian Legal Amazon', *Applied Geography*, vol. 140, 102651. <https://doi.org/10.1016/j.apgeog.2022.102651>

[Link to publication on Research at Birmingham portal](#)

General rights

Unless a licence is specified above, all rights (including copyright and moral rights) in this document are retained by the authors and/or the copyright holders. The express permission of the copyright holder must be obtained for any use of this material other than for purposes permitted by law.

- Users may freely distribute the URL that is used to identify this publication.
- Users may download and/or print one copy of the publication from the University of Birmingham research portal for the purpose of private study or non-commercial research.
- User may use extracts from the document in line with the concept of 'fair dealing' under the Copyright, Designs and Patents Act 1988 (?)
- Users may not further distribute the material nor use it for the purposes of commercial gain.

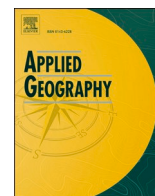
Where a licence is displayed above, please note the terms and conditions of the licence govern your use of this document.

When citing, please reference the published version.

Take down policy

While the University of Birmingham exercises care and attention in making items available there are rare occasions when an item has been uploaded in error or has been deemed to be commercially or otherwise sensitive.

If you believe that this is the case for this document, please contact UBIRA@lists.bham.ac.uk providing details and we will remove access to the work immediately and investigate.



Cloud cover and its impact on Brazil's deforestation satellite monitoring program: Evidence from the cerrado biome of the Brazilian Legal Amazon

Vilane G. Sales^a, Eric Strobl^a, Robert J.R. Elliott^{b,*}

^a University of Bern, Switzerland

^b University of Birmingham, UK

ARTICLE INFO

Keywords:

Remote sensing
Survival analysis
Environmental policies
Forest disturbance

ABSTRACT

The creation of a satellite rapid alert programme (DETER-A) in 2004 was a cornerstone of the Brazilian government's strategy to reduce deforestation. This programme allowed authorities to detect and respond rapidly to periods of deforestation. Due to the fact that the policy instrument was based on multispectral remote radar, weather-related obstacles posed a continuous impediment to the study of deforestation. This paper investigates to what extent cloud cover has reduced the effectiveness of the DETER-A program to detect deforestation. To test this hypothesis, survival model analysis is undertaken on satellite data derived measures of local deforestation. The emphasis is on the state of Maranhão, which is separated into two areas by an arbitrary line of demarcation (Legal Amazon delimitation) where the forest on one side is covered by the satellite monitoring program while the other is not. The results suggest that following the implementation of the satellite monitoring program, there was more deforestation in those years with more cloud persistence in the area covered by the program. Counterfactual simulations indicate that the absence of clouds would have prevented deforestation equivalent to almost 7% of the study region, which is equivalent to 73 million tonnes of CO₂ with a value of US\$ 366 million. If the current monitoring system was replaced with the experimental policy instrument DETER-C/DETER INTENSO, cloud cover would be less of an impediment to deforestation detection.

1. Introduction

The clear-cutting of forests plays a central role in many of the environmental threats of our time, including global climate change, habitat degradation, and species extinction. Although a global problem, nowhere are these issues more clearly on display than in the Brazilian Amazon that has seen the loss of 19 percent of its forest over the last 50 years. One bright spot has been the decline in deforestation rates in Brazil over the last decade, although there has been a resurgence in recent years. It is generally believed that the reduction in deforestation rates has been driven by a series of environmental policies that encouraged both forest preservation and the enforcement of existing regulations (Assunção et al., 2020; Celentano et al., 2017; Lovejoy & Nobre, 2018; Nepstad et al., 2014; Rajão et al., 2021; Richards, 2015; Richards & VanWey, 2015).

Arguably, the policy that has received the greatest plaudits is the satellite monitoring program that, through the use of remote detection, was able to considerably increase the speed by which the Brazilian environmental enforcement officers could punish clear-cutting agents.

More specifically, in 2004, the Brazilian government created the Action Plan for the Prevention and Control of Deforestation in the Legal Amazon (PPCDAm in Portuguese), the purpose of which was to pay closer attention to development planning, land use control, environmental law compliance, and the promotion of sustainable practices. To control land use and prevent further deforestation, the PPCDAm implemented two complementary satellite-based monitoring programs: (i) PRO-DES (Programa de Cálculo do Desflorestamento da Amazônia in Portuguese) (INPE, 2020) which records the annual rate of deforestation within the policy area using a high (30m) resolution; and (ii) DETER (Sistema de Detecção de Desmatamento em Tempo Real in Portuguese), which is a system that supports the supervision and control of deforestation and forest degradation within the environmental policy area of the Legal Amazon throughout the year but at a more moderate (250m) resolution.

The DETER system works by providing alerts when certain areas of the Legal Amazon are in the process of being deforested from relatively mild degradation to the total deforestation of an area (clear-cut). All data gathered by DETER and PRODES are available to the Brazilian

* Corresponding author.

E-mail address: r.j.elliott@bham.ac.uk (R.J.R. Elliott).

<https://doi.org/10.1016/j.apgeog.2022.102651>

Received 29 August 2020; Received in revised form 28 December 2021; Accepted 21 January 2022

Available online 10 February 2022

0143-6228/© 2022 The Authors. Published by Elsevier Ltd. This is an open access article under the CC BY license (<http://creativecommons.org/licenses/by/4.0/>).

government to enforce the PPCDAm, which includes the issuing of fines for agents who clear or damage the forest, embargoes on produce from areas that are in the process of being cleared, confiscation of equipment, and restrictions on access to subsidised credit (Aubertin, 2015).

While DETER has certainly allowed for much quicker detection of deforestation, a potentially important impediment to its success has been the local climate. More specifically, because the satellite used as part of DETER is incapable of detecting land cover changes when its view of the land surface is obscured by clouds, detection is necessarily delayed until the skies are clear again. The existing literature has already highlighted concerns regarding cloud cover. For example, Butler and Moser (2007) showed that estimates of deforestation and studies that use deforestation data from satellite images could potentially be biased without the proper corrections for cloud cover. In addition, Hansen and Loveland (2012) and Leinenkugel et al. (2014) confirmed that seasonality and cloud cover reduce the viability of annual land cover updates, and, consequently, systematic monitoring. Likewise, Dupuis et al. (2020) discusses how new satellite technologies can help with monitoring forest degradation in the presence of significant cloud cover. Recently, Nicolau et al. (2021) substantiate the discussion by analyzing the applicability of Synthetic-aperture radar (SAR) methodology as a way of differentiating between modified land uses, which is ideally what is needed for early-warning deforestation systems.

In terms of the Brazilian Amazon, the role played by clouds is highlighted by Assunção et al. (2017) who show that cloud cover is an important predictor of the number of fines issued for deforestation within a given municipality. This is not surprising since, according to Mueller (2016) and Assunção et al. (2017), Brazil's institutions are setup in such a way that law enforcement agents can more easily punish offenders for illegal forest clearing if they are able to catch the perpetrators red-handed. The corollary is that, although in principle previous acts of deforestation can be legally punished, it is difficult to implement fines *ex post* because land and property rights are often unclear. The geography of the Brazilian Amazon also makes it particularly challenging for the police to access the highlighted areas since many of the illegal roads that provide access to virgin forest are deliberately built in such a way as to hamper enforcement agents (Pfaff et al., 2007).

Despite the potentially important role played by cloud cover in reducing the effectiveness of the DETER detection program launched in 2004, there is, to date, no study that explicitly examines the extent of this problem. To fill this gap in the literature, this study investigate whether cloud cover impairs the efficacy of the DETER detection programme. This study focuses on the state of Maranhão which has the unique property that it is divided by an artificial line of demarcation that separates it into two distinct regions: the Legal Maranhão (LM) and the Cerrado Maranhão (CM). This division, located at approximately 44° west of the meridian, means that the state has two areas that are both geographically similar (in terms of topography and forest cover) and are subject to the same municipality and state-level institutions and policies. The only discernible difference is that the area on one side of the line of demarcation is subject to the satellite monitoring system and the other is not. This presents a unique empirical setting in which it is possible to investigate whether the effect of cloud cover on deforestation differs between the two areas either side of this spatial division. More precisely, because forests located in the Cerrado Maranhão were not covered by the satellite monitoring program, under the hypothesis that cloud cover changes the behaviour of illegal loggers, there should be no such role for cloud cover in patterns of deforestation other than for climatic reasons (which would be the same for both sides of the demarcation line).

Importantly for this study, the forested areas on both sides of the border are fairly homogeneous in terms of biota and climate, with the only difference being the monitoring program implemented in the LM region. The closer to the border, the more similar the biota. To identify local deforestation and cloud cover within the two regions, remote sensing sources (MapBiomas Collection 5 and MODIS Land Cover Product) are used to construct a time event dataset at the individual

pixel level (250m × 250m) for the period of 2001–2016. Survival estimation methods are then employed to quantify the role of cloud cover on local deforestation events in both regions. Finally, the estimates from the survival analysis are used to simulate the effects of the monitoring programme and cloud cover under a number of different counterfactual scenarios.

2. Environmental policy: DETER-A monitoring system

DETER, which was established in 2004, is a support system for the inspection and control of deforestation and degradation in the Brazilian Legal Amazon and part of the Action Plan for the Prevention and Control of Deforestation in the Legal Amazon (PPCDAm) (West & Fearnside, 2021). The warnings indicate areas that have been completely deforested (clean cut) as well as areas that are experiencing forest degradation (e.g. logging, mining, and fires). The DETER System development plan (Near Real-Time Deforestation Detection) may be divided into three phases based on the resolution sensors deployed over time. In the first resolution phase (DETER-A) from 2004 until the end of 2017 it was used to produce alerts with a minimum mappable area of 25ha utilising images from MODIS sensors aboard NASA's TERRA and WFI satellites, as well as the Brazilian CBERS-2B satellite (INPE-DETER, 2018; Souza et al., 2019). The second phase started in 2015 (DETER-B) and used data from the AWiFS (Advanced Wide Field Sensor) sensor aboard the RESOURCESAT 2 satellite, which has a spatial resolution of 56 m and therefore allows monitoring with a minimum mapping area of 3 ha (Diniz et al., 2015). The third resolution stage (DETER-C or DETER INTENSO) combined optical images from the CBERS-4 (WFI and MUX), Landsat 8 (OLI), Sentinel 2 (MSI), and Sentinel 1 (C band) satellites with images from the Sentinel 1 SAR sensor to detect changes in forest cover in specific areas of the Legal Amazon, allowing for the detection of alerts larger than 1 ha. As of the date of publishing, the system is still integrating and validating its results, which are intended for inspection bodies only, and therefore the data is not yet publicly accessible.

During the period 2004 to 2016, the monitoring system in place (DETER-A) sent deforestation alerts every two weeks for inspection assistance and were forwarded to the environmental police (IBAMA) and to the environmental agencies of each individual state in the Legal Amazon. The DETER-A monitored forest areas in accordance to the RADAMBRASIL (1976) project in which included, among others, areas of Ecological Tension (forest/cerrado contact), with a predominance of physiognomy forestry. The information contained in these alerts enabled both groups to plan their field operations to combat illegal deforestation. The alerts were also combined into a monthly report that was made available to the general public. More precisely, because of cloud cover, the public reports were only available on a month by month basis for the period between May and October (when cloud cover is at its lowest) and quarterly between November to April (when cloud cover is at its greatest). Since the satellite system used by DETER-A was incapable of detecting land cover changes in areas covered by clouds, no forest clearing activity could be identified during these periods, and thus no alerts could be issued to pinpoint the location of degradation activity for that place and time (Assunção et al., 2017).

In addition, it is possible that the DETER-A instrument followed the same nonlinear policy path presented in the PPCDAm. As noted by West and Fearnside (2021), between 2004 and 2008, the Amazon experienced a significant decline in deforestation rates, which can be attributed to the DETER-A program and in part to economic factors such as commodity prices and currency exchange rates that affect the profitability of agricultural exports. From 2009 until 2011, the PPCDAm focused on the promotion of a sustainable development agenda for the Amazon forest, such as technical assistance and rural extension and sectoral agreements. Another major shift was the rise in the value of penalties and other environmental punishments mandated by Decree No. 6514 of 2008, as well as the restriction of equipment used to cause environmental harm, allowing for the rapid decapitalization of environmental

offenders. In 2012, the new Forest Code was adopted under the argument that the old regulation was unenforceable. With the new Forest Code 58 percent of all unlawful deforestation committed up to July 22, 2008, was pardoned, with tax assessments for individuals who deforested prior to that date being rejected. This approach significantly increased the feeling of impunity, creating an incentive for illegal deforestation and despite attempts to rein down deforestation, the trend began increasing again (Brançalion et al., 2016; Rajão et al., 2021; West & Fearnside, 2021).

3. Materials and methodology

3.1. Study area

The research region covers 34,401 square kilometres and comprises 21 municipalities. The sample includes only municipalities that are crossed by the 1953 line of demarcation at about 44° west of the meridian and have some territory on both sides. The line was initially established to allow the Brazilian government to plan the economic growth of the region, which includes the Maranhão state's tropical forest region. The strategy was intended to guarantee the occupancy of the land to the left of the line in order to expand the Amazon region's development potential and contribute to the establishment of a stable and progressive society in the Amazon. It is the only state in Brazil with this kind of policy border. Importantly, state-level institutions, rules, regulations, and policies are the same on both sides and have been utilized to delimit the coverage of the DETER-A instrument. The delimitation is shown in Fig. 1.

In the study area, the average percentage of the sky that is covered by clouds is subject to extreme seasonal variation. The period when there is the least amount of cloud cover in Maranhão is between June and October. In July, the sky remains cloudless, almost cloudless, or partly overcast for more than 65% of the time and overcast for 35% of the time. The cloudiest period begins around October and lasts around 7–8 months, ending around June. In April, the sky remains cloudy or mostly cloudy for more than 80% of the time and cloudless, almost cloudless, or partly cloudy for less than 20% of the time. The evolution of cloud cover over the year is shown in Fig. 2. Understanding how climatic conditions change throughout the year helps with an understanding of the dynamics of deforestation in the region. With a rainy season that lasts almost nine months, the dry season is limited to the remaining three months of the year, June, July, and August, when there is good satellite visibility across the entire area.

One possible concern with a number of empirical studies on the causes and consequences of deforestation is that it has been shown that for parts of the Amazon forest, cloud formation depends on the topography of the location (Chagnon et al., 2004; Heiblum et al., 2014; Koren et al., 2004; Pinto et al., 2009; Wang et al., 2009). More precisely, the evapotranspiration characteristics of land cover vegetation are intimately related to the dynamics of the boundary layer and the development of clouds that often cap the boundary layer. As a consequence, compared to heavily wooded regions, deforested areas in the Amazon (when replaced with pasture or farmland) are more likely to have greater sensible heat and lower latent heat fluxes. This may increase the boundary layer's development throughout the day and therefore favour the production of bigger clouds. In other words, deforested regions promote cloud formation. The difficulty for academics is to determine whether the presence of clouds promotes deforestation or whether prior deforestation facilitates cloud formation. However, the empirical design employed in this study alleviates these issues by concentrating on the ecological stress zone of Maranhão, a region devoid of thick forest, which implies that cloud formation over adjacent wooded areas or neighbouring deforested areas is not a problem. Instead, the ecological tension zone enables clouds to spread evenly throughout the region, thus excluding deforestation's reverse causality impact on cloud production but maintaining the applicability as it is considered a forest formation

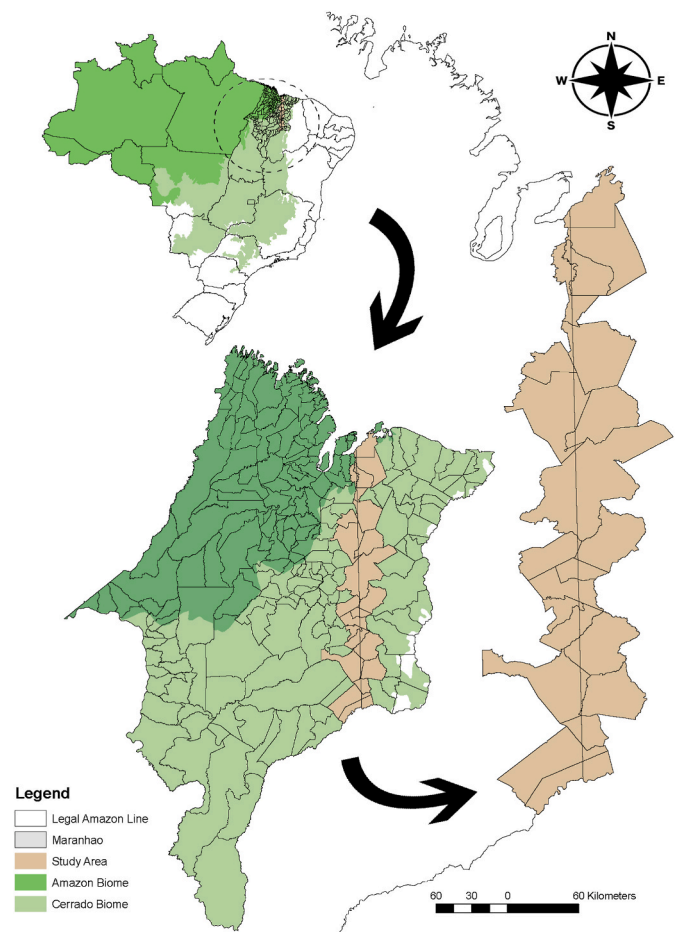


Fig. 1. Map of Maranhão including forest formation and institutional delimitation. The vertical line is the institutional division of the Legal Amazon in the State. Forest Formation includes Amazon biome and Cerrado biome classification. Map created by authors with data from MMA (2018); NUGEO (2018); F. G. Assis et al. (2019).

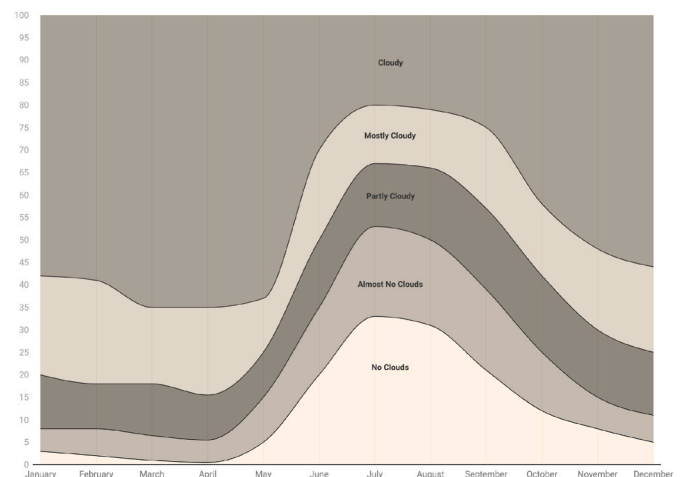


Fig. 2. Cloud Cover Dynamics in Maranhão. The plot represents the percentage of cloud cover in the state over 12 months. Map created by authors with data from INPE (2020).

for the monitoring instrument.

3.2. Cloud cover mask

Two remotely sensed datasets were used – Vegetation Indices 16-Day L3 Global 250m MODIS13Q1 and Land Cover Type Yearly L3 Global 500m MODIS12Q1. The MODIS Land Cover Type Product (MCD12Q1) provides a diverse classification Land cover scheme. The MODIS Vegetation Indices (VI) (MOD13Q1) product consists of time series comparisons of global vegetation conditions and cloud cover persistence. Two masks were derived from the products, namely, the Land Cover mask and Goodness of Fit mask. The Land Cover mask was utilized to select only forested pixels according to the classification of the University of Maryland (UMD). A complete list of the classes and their definitions can be found in [Setiawan et al. \(2014\)](#); [Sulla-Menashe and Friedl \(2018\)](#). After applying the Land Cover mask to the VI images, the Goodness mask was used to select pixels that were reported as being covered by clouds. With the goodness mask results, an image from the first and second 16-day periods that contains only cloud-marked pixels was created and these were then summed for all months to calculate the number of months in a year when a pixel is flagged as cloudy. The next stage was to perform a Kernel Regression of the share of deforested pixels against the number of periods with cloud cover to check the threshold period for cloud cover persistence for the study period. The optimal bandwidth used was the one suggested by [Bowman and Azzalini \(1997\)](#) with 1000 replications and with cross-validation. Seventeen cross-validated kernel regressions were estimated. The results of the regressions suggested a threshold of approximately five months.

The final cloud mask was applied to all annual images using the identified threshold. If the pixel's cloud cover value was equal to or more than the threshold within a year, it was reported as a cloud cover pixel and a dichotomous variable was created. In addition, the same approach described above was used to create a monthly cloud cover data set. However, instead of implementing a kernel regression, the exact month in which the pixel was covered by a cloud was tabulated. All regressions exhibited a consistent pattern of outcomes. As a consequence, the primary findings section presents the analysis on the outcome of the threshold selection highlighted. The resulting data set consists of a binary variable indicating whether or not a pixel was flagged as clouded according to the threshold.

3.3. Deforestation dataset

The study collected deforestation information from the Brazilian-based annual land use and land cover mapping project (MapBiomias Collection 5). This dataset reconstructs yearly land use and land cover (LULC) information at 30-m spatial resolution for every Brazilian biome from 1985 to 2019 using a random forest algorithm applied to the Landsat archive and Google Earth Engine ([Project, 2021](#); [Souza et al., 2020](#)). The MapBiomias initiative emerges as a novel tool for studying forest dynamics in the extremely heterogeneous study region by combining medium-resolution remote sensing data with a comprehensive land use classification. The mosaic of images is composed of the best pixels from all images available during a specified period within a year. After defining the start and end dates of this period, the median of the pictures captured during that time period was computed, yielding one median value per pixel per year. The window period used in the MapBiomias dataset corresponds to the period of April to September ranging from 60% to 30% of cloudy days according to [Fig. 2](#). The legend categories of the yearly deforestation maps were aggregated into two categories: “deforested” and “not deforested”. The study also included a binary land cover map of “forest” and “not-forest” to filter out of the deforestation map land cover classifications that do not belong to the biome.

Notably, a temporal gap fill filter was used to account for the absence of data values (gaps) caused by cloud-covered (or cloud shadow) pixels

in a given picture. The filter consistently filled in the gaps using the classification of the chronologically nearest future valid event. If no future valid classification could be determined, the no-data value was replaced with its prior valid classification. To account for cloud cover, the deforestation dataset was superimposed over the cloud mask dataset. A postclassification temporal filter based on a moving window was also applied to simplified maps to reduce uncertainty and year-to-year fluctuations in native forest loss and growth ([Nanni et al., 2019](#)). Hence,

$$Suppression_t = \begin{cases} F_{t-2} \\ F_{t-1} \\ A_t \\ A_{t+1} \end{cases} \quad (1)$$

where F corresponds to Forest as a class of vegetation (Forest Formation, Savanic Formation), A corresponds to any class of Anthropogenic use and $t = 2000, \dots, 2016$ taking 2000 as the base year. When a pixel was classified as “Forest” for at least two years and then “Anthropic” for at least two years, the algorithm considered it to be part of a deforestation episode ([Souza et al., 2020](#)).

The dataset was aggregated from a 30-m resolution to a 250-m resolution using reproject and resampling tools from the Google Earth Engine ([Gorelick et al., 2017](#)). This is vital for the analysis because it allows, for example, a comparison of 30-m pixels from a Landsat-based deforestation analysis to coarse pixels from the MODIS-based cloud cover mask. For the investigated area, the final data set consists of a binary variable denoting deforested pixels (1) and forest pixels (0) matched by unique IDs to the final dataset of Cloud Cover.

3.4. Risk factors

Numerous studies demonstrate that a variety of factors may influence deforestation patterns and are suspected as risk factors that can cause a shift in the trend ([Arima et al., 2014](#); [Rochedo et al., 2018](#); [Soares-Filho et al., 2006](#)). To account for these factors, information was gathered from a variety of sources to create a distance-based set of risk factor covariates that are described in [Table 1](#). To determine the distance between each pixel and the covariates, the data were converted into a raster format and the Euclidean distance between each pixel and the variable source within the research area was calculated. Roads, protected areas (PA), regional markets, city centres, and mines were the source variables measured in 2000. The Euclidean distance between a certain pixel and a river basin was used (but no transformation was needed). Time-varying variables were calculated for each year of the study period as the percentage of adjacent pixels that are forested. Annual averages of rainfall and temperature are also included. Latitude, longitude, and elevation are calculated at the pixel level. In addition, factors influencing the trend in deforestation were created, such as identifying the DETER-A policy's presence and the persistence of clouds in a specific pixel.

3.5. Survival models

Let n be the total number of pixels and $t_{(j)}$ is the time under study for the j th pixel. $\delta_{(j)}$ is the deforestation indicator, where $\delta_{(j)} = 1$ for deforestation and $\delta_{(j)} = 0$ if the pixel is right-censored, i.e., it is not possible to calculate the pixel real survival period because the study period ended and the pixel had no evidence of deforestation). $X_{(j)}$ is a vector of risk factors for the j th pixel that may affect the distribution of X , the time it takes to deforest.

Let $\lambda(t|X)$ be the hazard rate in the subpopulation with covariate value X . The Cox proportional hazard regression model relates covariates to the hazard function as follows:

$$\lambda(t|X) = \lambda_0(t)\exp(\beta' \cdot X) \quad (2)$$

Table 1
Data description.

Variable	Source	Description	Source Data Type	Source Resolution
PA	MMA	Euclidean distance to the nearest protected area in decimal degree.	Polygon	–
Mine	EMBRAPA	Euclidean distance to the nearest mineral resource/mining in decimal degree.	Point	–
Market	CONAB	Euclidean distance to the nearest regional market in decimal degree.	Point	–
Municipality	IBGE	Euclidean distance to the nearest municipality centre in decimal degree.	Point	–
River	IBGE	Euclidean distance to the nearest river/basin in decimal degrees.	Polyline	–
Road	IBGE	Euclidean distance to the nearest road in decimal degrees.	Polyline	–
Elevation	EMBRAPA	Digital elevated map of Maranhão.	Raster	30m
Latitude and Longitude	IBGE	latitude and longitude of each pixel in the study. This is used to account for spatial autocorrelation across large distances.	Raster	250m
Rainfall and Temperature	BDMEP/ INMET	historical series of several conventional meteorological stations of the INMET station network.	Point	–

where $\lambda_0(t)$ is the baseline hazard function and $\beta' = (\beta_1, \beta_2, \dots, \beta_p)$ is a vector of regression coefficients. This model is semi-parametric since the baseline hazard model is estimated non parametrically, while the risk factors are constrained by the parametric representation $\exp(\beta' \cdot X)$. The parametric function is assumed to take the exponential form $\exp(\beta' X) = \exp(\sum_{k=1}^p \beta_k X_k) = e^{\sum_{k=1}^p \beta_k X_k}$. The Cox model is a proportional hazard model in the sense that the ratio of the hazard function at time t does not depend on t and the hazard rates are proportional (Cao, 2005; Lee & Wang, 2003) and is given by:

$$\frac{\lambda(t|X_1) = \lambda_0(t)\exp(\beta' \cdot X_1)}{\lambda(t|X_2) = \lambda_0(t)\exp(\beta' \cdot X_2)} = \exp(\beta'(X_1 - X_2)) \tag{3}$$

Time-varying covariates are introduced to the model to compensate for possible unobserved spatial and temporal heterogeneity:

$$\lambda(t|Z(t)) = \lambda_0(t)\exp(\beta' x + \gamma' X(t)) \tag{4}$$

where β' and γ' are the coefficients of time-invariant and time-varying covariates, respectively. Letting $Z(t)$ represent the time-varying covariates, then:

$$Z(t) = [x_1, x_2, \dots, x_p, X_1(t), X_2(t), \dots, X_q(t)] \tag{5}$$

Hence, the hazard ratio can be written as:

$$\widehat{HR} = \left(\frac{\lambda(t; Z(t))}{\lambda(t; Z(t)^*} \right) = \exp(\beta' x^* + \gamma' X(t)^*) \tag{6}$$

which is a nonconstant hazard. One way to model coefficients that vary significantly over time is to use a step function, $g(t) = I(t \geq t_0)$, where t_0 has a specified value. The idea is to split the analysis of time into several intervals so that the Cox proportional model is stratified for these time intervals. As previously mentioned, the DETER-A instrument is likely to have followed a similar nonlinear policy course as the PPCDAm. Thus, the strategy stratifies the survival model over three distinct time periods to rule out nonlinear outcomes hindered by the dichotomous variables. According to the literature, the phases are as follows: (1) the policy implementation phase (2004–2008); (2) the sectoral agreements phase (2009–2011), and; (3) the new Forest Code implementation phase (2012–2016).

In general, relative hazard values greater than one indicate a positive impact of the risk factor, i.e., it increases the probability of deforestation. Values less than one imply a negative impact on deforestation. A set of controls are included: A policy coverage dummy (Policy), that is, one from 2004 onwards and zero otherwise for the standard model and a stratified policy dummy with 3 intervals (2004–2007, 2008–2011, 2012–2016); cloud cover dummy created from the cloud cover mask (Clouds); a Legal Maranhão indicator (LM); interaction terms capturing (1) the role of cloud cover during those years when the policy was operating (Policy*Clouds) and (2) for the whole period of the study (Clouds*LM) regardless the implementation of the policy.

3.6. Counterfactual analysis

Counterfactual analysis were conducted to determine how much forest would have been lost in the absence of policy or clouds by comparing the total marginal probabilities of two distinct scenarios. This calculation utilises an Augmented-IPTW model (AIPTW). The AIPTW estimator is doubly robust in which one model forecasts the treatment (in this case, IPTW) and another model predicts the outcome (like the g-formula) Funk et al. (2011).

The estimator only takes into consideration the time that a pixel is deforested, and it considers that a pixel is deforested if its difference in the probability of survival is positive. The IPTW technique creates a pseudopopulation in which the average causal effect of the treatment $A = (0, 1)$ (clouds and policy) on the time to deforest $\delta_{(j)}$ is identical to the observed population's average causal effect. In the pseudopopulation, the set of risk factors, X , is no longer related to the clouds and policy variables, i.e., the covariates are unrelated to treatment assignment. Pixels in the pseudopopulation are weighted according to their treatment probabilities. If a pixel j is covered by clouds or within the policy area, its weight is one over its probability of $A = 1$ (based on its covariates). If the pixel j did not receive the treatment, $A = 0$, their weight is one over their probability of receiving the control. Therefore, treated pixels who were less likely to be treated have larger weights, as do the control pixels who were less likely to receive the control, thus creating a balanced pseudopopulation. On the other hand, the g-formula enables the identification of the marginal value of a possible outcome for $\delta_{(j)}$ under treatment $A = a$, i.e. the counterfactual scenario ($\delta_{(j)a}$), under the identifiability assumptions. The estimator then combines these estimates in such a way that if either specification is valid, the estimate is consistent. Given that Cox model is estimated consistently, the Augmented-IPTW (AIPTW) consists of the following:

$$E[\delta^a] = \frac{1}{n} \sum_i^n \left(\frac{\delta * I(A = a)}{\widehat{\Pr}(A = a|X)} - \frac{\widehat{E}[\delta|A = a, X] * (I(A = a) - \widehat{\Pr}(A = a|X))}{1 - \widehat{\Pr}(A = a|X)} \right) \tag{7}$$

where $\widehat{\Pr}(A = a|X)$ comes from the IPTW model and $\widehat{E}[\delta|A = a, X]$ comes from the g-formula.

3.7. Cost-benefit analysis (CBA)

CBA is employed to assess the impact of the DETER-A instrument and the degree to which cloud cover affects the policy's efficacy in the battle against deforestation. The analysis is then expanded to assess the effect in terms of CO₂ emissions. The CBA is done by comparing the total of Ibama's and INPE's annual budgets with the counterfactual outcomes of the estimated monetary benefits of maintaining forested areas and therefore avoiding carbon dioxide emissions. The estimated values are based on the conversion factor of 10,000 tC/km² (36,700 tCO₂/km²), as determined by the Ministry of the Environment MMA (2018) and the price of 5 USD/tCO₂/km² commonly used in current applications. This

approach was taken in this paper so the estimates are comparable with those of the Ministry of the Environment.

3.8. Validation

The study is predicated on the buffer zone established either side of the artificial line to isolate and compare pixels being geographically and physiologically homogeneous. To establish support for this critical assumption, an effect size index is produced for the two regions on either side of the line following Cohen (1977) who computed and represented variations in means in terms of the pooled within-area standard deviation. The Cohen index is interpreted in terms of the average percentile standing area compared to another. To assess the sensitivity of our choice of buffer zone, we also replicated the results after a 0.2° increase in the buffer zone.

To validate the survival analysis results, a concordance index, commonly known as the c-index, which assesses the precision with which the anticipated time is ordered, is employed. This is a generalisation of the AUC (area under the curve), another often used loss function, and is interpreted identically (Davidson-Pilon et al., 2018). More precisely, a c-index of around 0.5 represents the predicted outcome of random predictions, whereas 1.0 represents perfect concordance and 0.0 represents perfect anti-concordance. In addition, k-fold validations are performed which entails splitting a training set from the data into k smaller sets ($k = 5$). A model is trained using $k - 1$ of the folds as training data. The resulting model is validated on the remainder of the data, i.e., it is used as a test set to compute a performance measure such as accuracy. The performance measure reported by k-fold cross-validation is then the average of the values computed in the loop and should be close to 0 (Pedregosa et al., 2011).

According to Souza et al. (2020), the deforestation dataset (Collection 5.0) was constructed using Random Forest models calibrated with training data drawn from the region with stable categorization during the 34-year period covered by the previous collection, as well as from Native Vegetation (NV) reference maps. The sample size was first fixed at 7000 per classification unit of forest type (Forest Formation and Savanna Formation (legend ID: 3,4)) and then divided proportionately across classes according to the area of each class using the year 2000 as the baseline. The minimum sample size was set at 700 to ensure that adequate samples were collected for classes that included less than 10% of a particular region. Independent classifications were created for the region in different years, and the resulting time series were post-processed using filters to improve temporal and spatial coherence. Visual examination of intermediate versions was used to detect if the region presented spatial discontinuities with neighbouring regions or regions with notable omission/commission mistakes for a particular class. These instances were reclassified using a modified sample size distribution per class, which was determined by an interpreter to account for the proportionate excess/deficiency of the area in a particular class in the assessed version.

The validation strategy was based on statistical techniques using independent sample points with visual interpretation across the study region (Amazonia/Cerrado) and time series. The accuracy study was conducted using the LAPIG dataset, which had around 50,000 reference sample pixels for the study region (Stehman, 2014). An impartial team evaluated the sites during the dry/wet season using a combination of Landsat and Google Earth data and the Temporal Visual Inspection tool (tvi.lapig.iesa.ufg.br). Each location was reviewed by three separate interpreters, and the legends were simplified to match those seen on yearly maps (See S1 for detailed information on the legend groups) (Olofsson et al., 2014). The confusion matrix was used to determine global and class-level accuracy, omission and commission errors, as well as quantity and allocation conflicts, by comparing the reference dataset to sample pixels from Collection 5's integrated version.

4. Results

4.1. Validation

The validation results include the Cohen index for the study area. The average is about 0.09, indicating that the mean of the LM region is at the 50th percentile of the CM region, implying that the distribution of scores for the LM region overlaps with the distribution of scores for the CM region, with effectively 0% of non-overlap and dissimilarity. Checking for the robustness assumption of a homogeneous study area, the Cohen index for the area not included in the study design by 0.2° was 0.28, indicating that the LM region is at the 62nd percentile of the CM region, rejecting the null hypothesis that these two regions are identical. Indeed, the index value of 0.28 shows a 21 percent difference between the two distributions, following Cohen (1977) methodology.

Validating the survival models, the c-index is equivalent to 0.511 (se = 0.003) for the standard model and 0.513 (se = 0.003) for the stratified model. The k-fold validation result for the standard model is equal to -0.35 (se = 0.001) and for the stratified model -0.34 (se = 0.001). The accuracy analysis of the MapBiomass dataset were carried out using the method described by Pontius and Millones (Pontius & Millones, 2011), and revealed an overall accuracy of 83 percent for the most detailed legend, with an 11.8 percent disagreement in allocation and a 5.2 percent disagreement in area, and consistent accuracy across the time series (See S1 for detailed information). The results for the study area are in line with the region's geographical and temporal deforestation pattern. The comparison between the original dataset (MapBiomass Collection 5) and the final deforestation dataset for the study is shown in the visual graph supplied in the S1 supplementary file.

4.2. Summary statistics

Table 2 provides the summary statistics for the survival rates and risk factor variables. The sample contains 550,428 observations for the time-varying model as well as eight risk factors and several other controls. The period of the study is 2000–2016 using the first year as the baseline. Overall, the average time a pixel is in the sample before it becomes deforested is 16 years. Around 41% of the pixels belong to the Legal Maranhão region and approximate 0.1% of the analysed pixels are deforested at some point during the sample period. Around 68% of the pixels were covered by clouds on two consecutive 16-day images at least for five consecutive months (capturing cloud persistence). Rivers and roads were the closest features to any given pixel, on average, with Protected Areas and regional market places being the furthest away.

Table 2
Descriptive statistics.

Variables	Mean	Std Deviation	Min	Max
Survival	16.968	4.129	1.000	17.000
Deforestation	0.001	0.198	0.000	1.000
Clouds	0.682	0.465	0.000	1.000
LM	0.411	0.492	0.000	1.000
Rainfall	83.433	35.366	19.500	189.500
Temperature	32.245	2.259	20.166	35.333
Forest	0.983	0.093	0.000	1.000
PAs	0.623	0.289	0.000	1.188
Mining	0.059	0.081	0.000	0.370
Market	0.327	0.188	0.000	1.087
Municipality	0.124	0.057	0.000	0.302
River	0.016	0.012	0.000	0.063
Road	0.046	0.042	0.000	0.212
Lat	-2.642	0.193	-3.003	-2.347
Lon	-40.839	1.040	-43.770	-39.586
Elevation	218.168	106.496	0.000	492.000

¹ Statistics refer to 550,428 observations. All distancing values are in decimal degrees.

² The conversion assumes 0.1° to 11 km².

Reassuringly, almost 98% of pixels were surrounded by other forested pixels to ensure that it is the forest that is being captured by the indices. Throughout the entire period, rainfall averaged about 83 mm and temperatures hovered around 32c per year.

4.3. Survival analysis

Table 3 shows the estimated effect of covariates on the hazard of any of the pixel observations becoming deforested, where the coefficients are given as hazard ratios. The relative hazard ratios (RHR) in the second column of Table 3 show that pixels in the Legal Maranhão (LM) were twice as likely to be deforested (RHR of 2.143) as pixels in the Cerrado Maranhão (CM). However, the implementation of the monitoring policy (Policy) reduced the probability of a pixel being deforested by almost 45% (RHR of 0.551). Although the policy reduced deforestation rates in the LM region, and in concordance with the hypothesis of this paper, cloud cover during the period of the policy (captured by the Policy*Cloud variable) reduced the effectiveness of the policy by 2.2 times compared to the CM region (RHR of 2.299). This result should be considered alongside the general finding that cloudy skies *per se* do not have an impact on the relative hazard ratio. This finding is substantiated by the magnitude of the effect of clouds on the Legal Maranhão for the whole period, which decreases the probability of deforestation by almost 66% (RH of 0.449 for the Cloud*LM interaction term).

The results from the survival analysis support the hypothesis that while the introduction of the satellite monitoring program significantly reduced the level of forest loss in the LM region relative to the Cerrado Maranhão, this coincided with an increase in deforestation in those years that experienced a higher prevalence of cloud cover. In terms of the other controls, an increase in the distance of one degree or 11 km of a mine from a pixel lowers the hazard ratio by 41% (RHR of 0.604), whereas being further from a road decreases the hazard by almost 62% (RHR of 0.482). In contrast, being further away from one of the major storage and trading markets (RH of 1.317) increases the probability of being deforested. The other controls had no significant impact on survival rates.

The stratification results of the three policy implementation periods are given in Table 4 by the relative hazard ratios (RHR) of the stratified covariates Policy and the interaction effect of Policy*Clouds. Policy had a nonlinear trajectory throughout the sample period, being only significant during the last phase of the policy analysis. The probability of a pixel being deforested between 2012 and 2015 decreased by 45% (RHR 0.550). When the cloud cover during the policy's implementation period

Table 3
Cox proportional hazard model time varying covariates.

Variables	Coef	RelativeHazard Ratio	StandardErrors	Z score
Clouds	-0.032	0.968	0.017	-1.881
Policy	-0.596***	0.551	0.207	-2.888
Policy*Clouds	0.833**	2.299	0.362	2.298
LM	0.762***	2.143	0.207	3.684
Clouds*LM	-0.801**	0.449	0.363	-2.210
PAs	0.135	1.145	0.087	1.561
Mining	-0.504***	0.604	0.111	-4.535
Market	0.276***	1.317	0.074	3.749
Municipality	0.040	1.041	0.120	0.335
River	-0.315	0.730	0.540	-0.583
Road	-0.730***	0.482	0.182	-4.001
Forest	0.012	1.012	0.051	0.236
Rainfall	0.000	1.000	0.002	0.165
Temperature	-0.246***	0.782	0.009	-27.791

Sample consists of 550,428 observations. **** denotes hazard ratios that are significantly different from 1 at the 99% (0.001) confidence level. *** denotes hazard ratios that are significantly different from 1 at the 95% (0.01) confidence level. PAs stand for Protected Areas (Indigenous Lands and Conservational Units). *LM stands for interaction with Legal Maranhão region. We include latitude, longitude and elevation as additional unreported controls.

Table 4
Cox proportional hazard model time varying covariates - stratified model.

Variables	Coef	RelativeHazard Ratio	StandardErrors	Z score
Clouds	-0.032	0.968	0.017	-1.881
Policy:(1)	-0.370	0.691	0.350	-1.056
Policy:(2)	0.013	1.013	0.365	0.036
Policy:(3)	-0.598***	0.550	0.206	-2.899
Policy*Clouds:(1)	1.188**	3.279	0.472	2.517
Policy*Clouds:(2)	0.332	1.394	0.492	0.675
Policy*Clouds:(3)	0.830**	2.292	0.362	2.289
LM	0.761***	2.143	0.207	3.684
Clouds*LM	-0.800**	0.449	0.363	-2.210
PAs	0.136	1.145	0.087	1.561
Mining	-0.504***	0.604	0.111	-4.535
Market	0.276***	1.317	0.074	3.749
Municipality	0.040	1.041	0.120	0.335
River	-0.313	0.730	0.540	-0.583
Road	-0.731***	0.482	0.182	-4.001
Forest	0.012	1.012	0.051	0.236
Rainfall	0.000	1.000	0.002	0.165
Temperature	-0.246***	0.782	0.009	-27.791

Sample consists of 550,428 observations. **** denotes hazard ratios that are significantly different from 1 at the 99% (0.001) confidence level. *** denotes hazard ratios that are significantly different from 1 at the 95% (0.01) confidence level. PAs stand for Protected Areas (Indigenous Lands and Conservational Units). *LM stands for interaction with Legal Maranhão region. We include latitude, longitude and elevation as additional unreported controls.

is taken into account (as shown by the Policy*Cloud variable), the significance is observed for two periods: the implementation of the policy and the new Forest Code. As can be shown, the policy's efficacy reduced by 3.2 to 2.2 times when compared to the CM region (RHR of 3.279 and 2.292, respectively), despite the fact that the effects diminished over time.

4.4. Counterfactual analysis

The survival model estimates are now used to run a series of counterfactual simulations. Under the no monitoring program scenario, it is predicted that there would have been an additional 1954 km² of the forest that would have been flagged as deforested. Given that the total area of the sample is the equivalent of 34,401.75 km², this implies that if the satellite monitoring program had not been implemented, *ceteris paribus*, the deforestation area would have covered almost 5.7% of the sample area. When allowing for the satellite program, but assuming that there was no disruption to monitoring due to clouds, the results indicate that the area of deforestation would have been reduced by 1995 km². The counterfactual survival model estimates suggested that almost 41 Km² of forests were cleared due to the presence of clouds, which corresponds to almost 0.14% of the study region.

4.5. Cost-benefit analysis

With the results above, a simple cost-benefit analysis is conducted based on the absence of the satellite monitoring program in the study region using counterfactual estimates. More precisely, with no monitoring, the estimated level of additional deforestation that would have occurred during the sample period would have consumed approximately 71 million tonnes of CO₂, which is equivalent to US\$ 358 million (at 2018 prices). For the scenario in which clouds no longer pose a problem for monitoring, estimates suggest that the newly preserved forest area could store an additional 73 million tonnes of CO₂ with a value of US\$ 366 million over the study period for the LM and CM regions.

5. Discussion

The survival analysis and counterfactual simulations indicate that deforestation is facilitated by an intricate relationship between illicit loggers, government regulators, technological advancements, and climatic circumstances. The narrative is mainly a positive one in that Brazil's implementation of the satellite monitoring programme (together with wider environmental laws designed to encourage the use of such technology) resulted in a reduction in deforestation in the Legal Maranhão.

However, at the same time, the results show that following the introduction of the monitoring program, those years where there was a greater degree of cloud cover saw a relative increase in the probability of deforestation. This suggests that cloud cover had a mitigating effect on the effectiveness of the monitoring programme. This is consistent with the decision of illegal loggers to change their behaviour and to undertake their illegal activities under the cover of clouds when the probability of being caught is likely to be substantially lower. The findings can also reflect a possible shift with illegal loggers moving their activities across the line that distinguishes the Legal Maranhão from the Maranhão Cerrado (where the monitoring program does not operate) (Pfaff & Robalino, 2017).

Regarding the policy instrument DETER-A, a nonlinear trend is found for the study region, indicating a significant decrease in the likelihood of deforestation between 2012 and 2016 compared to the period of the policy implementation phase. This period highlights the implementation of the New Forest Code, under which 58 per cent of all unlawful deforestation committed up to July 22, 2008, was granted amnesty, with tax assessments disallowed for individuals who deforested prior to that date. Prior to 2008, a significant portion of the infraction notices for damages to flora was suspended, totalling 28 thousand notices worth R\$ 4.8 billion. This strategy significantly increased the sense of impunity, creating an incentive for illegal deforestation. Fortunately, the inspection authorities took steps to address the increased pressure caused by deforestation. In addition, the banking industry was singled out for giving rural loans to manufacturing in an area that had been unlawfully deforested. The goal was to maximise the deterrent capacity of people who buy or finance products from illegally deforested areas at the lowest possible cost, to encourage market-based behaviour change (Rajão et al., 2021).

In terms of the other covariates, it is reassuring that their estimates are generally consistent with the previous literature. More specifically, the results show that the further the area of forest is away from a road, a river, or a mining concession, the less chance that trees in a given pixel have been deforested. This is consistent with the fish bone style pattern of deforestation that is often seen in images of Brazilian deforestation (Pfaff, 1997, 1999; Pfaff et al., 2007). Likewise, pixels close to a river are those that are most likely to be deforested, arguably because it makes transporting the logs to the market much less costly than moving them across land. This is consistent with the common image of substantial numbers of logs floating down the river to be picked up, processed, and sold downstream. In terms of human settlement, the closer a pixel is to a regional market, the probability of deforestation falls as a result that is consistent with there being a stronger police presence in these areas.

Turning to the counterfactual simulations, it was shown that without a monitoring programme, almost 2000 km² of forest would have been categorised as deforested in the study region. This is a significant finding since, in the absence of the policy, the likelihood of the Legal Amazon becoming a savanna ecosystem would have been considerably greater (Lovejoy & Nobre, 2018). The cost benefit analysis indicated that under no monitoring, the estimated level of consumed CO₂ would surpass 71 million tonnes, which is worth roughly US\$ 360 million (in 2018 prices). This is crucial not just for the investigated area, but also for the Amazon forest, since the Brazilian Cerrado/Amazon transitional forests act as natural barriers of protection to the Amazon forest (Costa & Pires, 2010; Lapola et al., 2011; Malhado et al., 2010; Morandi et al., 2016).

Moreover, the implementation of a more technologically advanced satellite system that can better deal with cloud cover was considered. An example of such a technology would be that carried out in the DETER-C/DETER INTENSO microwave domain, since microwaves have the ability to penetrate through clouds and are very useful for the detection of deforestation in real time (Dupuis et al., 2020; Nazarova et al., 2020). In addition, the existing efforts of the DETER-B instrument to detain deforestation by increasing image resolution and temporal path combined with machine-learning-based cloud detection methods, such as neural networks and support vector machine algorithms, can extract more robust and high-level information from optical sensors, such as MODIS and Landsat satellites, within a reasonable testing time. In fact, from 2017 to 2019, DETER-B alerts were able to account for approximately 40% of total deforestation in the state of Maranhão.

Nonetheless, the supposed battle against deforestation is far from over and rates of deforestation have been increasing in recent years. Apart from climatic barriers, federal inspection is in danger owing to a shortage of people and financial resources, as well as changes in environmental and penal legislation that provide flexibility for offenders or render operations impossible (Zi et al., 2018; F. G.; Assis et al., 2019; Rajão et al., 2021; Valente, 2021). One concerning aspect of these findings is that, in a recent study by Matricardi et al. (2020), it was observed that forest degradation has overtaken deforestation in the Brazilian Amazon from 1992 to 2014, and this article does not clearly address or analyse this fact. It is recognised that the results may underestimate the real casual influence of clouds on the policy instrument.

6. Conclusion

The state of Maranhão provides an ideal setting in which to study the impact of clouds on the behaviour of illegal loggers as the state is divided by an artificial line that separates it into two parts. To the left of the line is the Legal Maranhão (LM) where the satellite monitoring DETER-A operates and to the right of the line the area called the Cerrado Maranhão (CM) where there is no monitoring. Other than that, both areas have the same institutions, rules, and laws. This study quantified the extent to which cloud cover inhibited the ability of the Brazilian satellite monitoring system to detect episodes of deforestation in the Brazilian Amazon using satellite-derived data and forest survival analysis estimation. The findings support the hypothesis that more deforestation occurs during years with higher cloud cover. In addition, the results indicate that improved satellite monitoring technologies, such as the DETER-C/DETER INTENSO testing phase policy instrument, may have a substantial effect on deforestation rates. Similarly, one might use improved techniques to identify vegetation in the presence of clouds, such as a new cloud identification approach for multispectral remote sensing images based on machine-learning algorithms (Zi et al., 2018).

Statement of contribution

Sales: Conceptualization; Data curation; Formal analysis; Funding acquisition; Investigation; Methodology; Resources; Software; Validation; Visualization; Roles/Writing - original draft;

Strobl: Conceptualization; Formal analysis; Investigation; Methodology; Project administration; Supervision; Validation; Writing - review & editing.

Elliott: Conceptualization; Project administration; Supervision; Writing - review & editing.

Acknowledgements

This work was undertaken with support from Coordenação de Aperfeiçoamento de Pessoal de Nível Superior (CAPES), Brazil, grant Doutorado Pleno no Exterior - Proc. BEX 2228/15-7. We also acknowledge support from the Birmingham Institute of Forest Research (BiFor) and Thomas Pugh and three anonymous referees for excellent

comments. Errors are our own.

Appendix A. Supplementary data

Supplementary data to this article can be found online at <https://doi.org/10.1016/j.apgeog.2022.102651>.

References

- Arima, E. Y., Barreto, P., Araujo, E., & Soares-Filho, B. (2014). Public policies can reduce tropical deforestation: Lessons and challenges from Brazil. *Land Use Policy*, *41*, 465–473. <https://doi.org/10.1016/j.landusepol.2014.06.026>
- Assis, F. G., F. L., Ferreira, K. R., Vinhas, L., Maurano, L., Almeida, C., Carvalho, A., Rodrigues, J., Maciel, A., & Camargo, C. (2019). Terrabrasilis: A spatial data analytics infrastructure for large-scale thematic mapping. *ISPRS International Journal of Geo-Information*, *8*, 513. <https://doi.org/10.3390/ijgi8110513>. URL: .
- Assunção, J., Gandour, C., & Rocha, R. (2017). DETERing deforestation in the amazon: Environmental monitoring and law enforcement. Technical report. *Climate Policy Initiative*. <https://climatepolicyinitiative.org/wp-content/uploads/2013/05/D-ETERing-Deforestation-in-the-Brazilian-Amazon-Environmental-Monitoring-and-Law-Enforcement-Technical-Paper-Feb2017.pdf>.
- Assunção, J., Gandour, C., Rocha, R., & Rocha, R. (2020). The effect of rural credit on deforestation: Evidence from the Brazilian Amazon. *The Economic Journal*, *130*, 290–330.
- Aubertin, C. (2015). Deforestation control policies in Brazil: Sovereignty versus the market. *Forests, Trees and Livelihoods*, *24*, 147–162. <https://doi.org/10.1080/14728028.2015.1017540>
- Bowman, A. W., & Azzalini, A. (1997). *Applied smoothing techniques for data analysis: The kernel approach with S-plus illustrations*. Oxford science publications. Oxford University Press.
- Brancalion, P. H., Garcia, L. C., Loyola, R., Rodrigues, R. R., Pillar, V. D., & Lewinsohn, T. M. (2016). A critical analysis of the native vegetation protection law of Brazil (2012): Updates and ongoing initiatives. *Natureza & Conservação*, *14*, 1–15. <https://doi.org/10.1016/j.ncon.2016.03.003>. URL: .
- Butler, J. S., & Moser, C. (2007). Cloud cover and satellite images of deforestation. *Land Economics*, *83*, 166–173. <https://doi.org/10.2307/27647759>. URL: .
- Cao, H. (2005). *A comparison between the additive and multiplicative risk models*. Ph.D. thesis. Faculté des sciences et de génie - Université Laval Québec.
- Celentano, D., Rousseau, G. X., Muniz, F. H., Varga, I. V. D., Martinez, C., Carneiro, M. S., Miranda, M. V., Barros, M. N., Freitas, L., & Narvaes, I. D. S. e. a. (2017). Towards zero deforestation and forest restoration in the Amazon region of Maranhão state, Brazil. *Land Use Policy*, *68*, 692–698. <https://doi.org/10.1016/j.landusepol.2017.07.041>
- Chagnon, F. J. F., Bras, R. L., & Wang, J. (2004). Climatic shift in patterns of shallow clouds over the Amazon. URL: *Geophysical Research Letters*, *31*, 4 <https://agupubs.onlinelibrary.wiley.com/doi/abs/10.1029/2004GL021188> <https://agupubs.onlinelibrary.wiley.com/doi/pdf/10.1029/2004GL021188>.
- Cohen, J. (1977). Statistical power analysis for the behavioral sciences. In J. Cohen (Ed.), *Statistical power analysis for the behavioral sciences* (pp. 1–17). Academic Press. <https://doi.org/10.1016/B978-0-12-179060-8.50006-2>. URL: <http://www.sciencedirect.com/science/article/pii/B9780121790608500062>.
- Costa, M. H., & Pires, G. F. (2010). Effects of Amazon and central Brazil deforestation scenarios on the duration of the dry season in the arc of deforestation. *International Journal of Climatology*, *30*, 1970–1979.
- Davidson-Pilon, C., Kalderstam, J., Kuhn, B., Zivich, P., Fiore-Gartland, A., Moneda, L., Parij, A., Stark, K., Anton, S., Besson, L., Jona, Gadgil, H., Golland, D., Hussey, S., Noorbaksh, J., Klintberg, A., Evans, N., Braymer-Hays, M., Lukas, ... Rendeiro, A. F. (2018). *Camdavidsonpilon/lifelines*: v0.14.6. URL: <https://doi.org/10.5281/zenodo.1303381>.
- Diniz, C. G., Souza, A. A. d. A., Santos, D. C., Dias, M. C., Luz, N. C. d., Moraes, D. R. V. d., Maia, J. S., Gomes, A. R., Narvaes, I. D. S., Valeriano, D. M., Maurano, L. E. P., & Adami, M. (2015). Deter-b: The new Amazon near real-time deforestation detection system. *Ieee Journal of Selected Topics in Applied Earth Observations and Remote Sensing*, *8*, 3619–3628. <https://doi.org/10.1109/JSTARS.2015.2437075>
- Dupuis, C., Lejeune, P., Michez, A., & Payolle, A. (2020). How can remote sensing help monitor tropical moist forest degradation? - a systematic review. *Remote Sensing*, *12*, 1087. <https://doi.org/10.3390/rs12071087>
- Funk, M. J., Westreich, D., Wiesen, C., Stürmer, T., Brookhart, M. A., & Davidian, M. (2011). Doubly robust estimation of causal effects. *American Journal of Epidemiology*, *173*, 761–767. <https://doi.org/10.1093/aje/kwq439>. URL: .
- Gorelick, N., Hancher, M., Dixon, M., Ilyushchenko, S., Thau, D., & Moore, R. (2017). Google earth engine: Planetary-scale geospatial analysis for everyone. *Remote Sensing of Environment*. <https://doi.org/10.1016/j.rse.2017.06.031>. URL: .
- Hansen, M. C., & Loveland, T. R. (2012). A review of large area monitoring of land cover change using Landsat data. *Remote Sensing of Environment*, *122*, 66–74. URL: <http://linkinghub.elsevier.com/retrieve/pii/S0034425712000314>.
- Heiblum, R. H., Koren, I., & Feingold, G. (2014). On the link between Amazonian forest properties and shallow cumulus cloud fields. *Atmospheric Chemistry and Physics*, *14*, 6063–6074. URL: <https://www.atmos-chem-phys.net/14/6063/2014/>.
- INPE. (2020). *Instituto nacional de Pesquisas espaciais*. National Institute for Spatial Research. <http://www.inpe.br/ingles/>. (Accessed 1 July 2020).
- Inpe-Deter. (2018). Deter — coordenação-geral de observação da terra. URL: <http://www.obt.inpe.br/OBT/assuntos/programas/amazonia/deter>.
- Koren, I., Kaufman, Y. J., Remer, L. A., & Martins, J. V. (2004). Measurement of the effect of Amazon smoke on inhibition of cloud formation. URL: *Science*, *303*, 1342–1345. arXiv:<http://science.sciencemag.org/content/303/5662/1342.full.pdf> <http://science.sciencemag.org/content/303/5662/1342>.
- Lapola, D. M., Schaldach, R., Alcamo, J., Bondeau, A., Msangi, S., Priess, J. A., Silvestrini, R., & Soares-Filho, B. S. (2011). Impacts of climate change and the end of deforestation on land use in the Brazilian legal Amazon. *Earth Interactions*, *15*, 1–29.
- Lee, E. T., & Wang, J. W. (2003). *Statistical methods for survival data analysis: Lee/survival data analysis*. Hoboken, NJ, USA: John Wiley & Sons, Inc.. <https://doi.org/10.1002/0471458546>. Wiley Series in Probability and Statistics.
- Leinenkugel, P., Wolters, M. L., Kuenzer, C., Oppelt, N., & Dech, S. (2014). Sensitivity analysis for predicting continuous fields of tree-cover and fractional land-cover distributions in cloud-prone areas. *International Journal of Remote Sensing*, *35*, 2799–2821. <https://doi.org/10.1080/01431161.2014.890302>. URL: <https://www.tandfonline.com/doi/full/10.1080/01431161.2014.890302>.
- Lovejoy, T. E., & Nobre, C. (2018). Amazon tipping point. *Science Advances*, *4*, eaat2340. <https://doi.org/10.1126/sciadv.aat2340>. URL: .
- Malhado, A. C. M., Pires, G. F., & Costa, M. H. (2010). Cerrado conservation is essential to protect the Amazon rainforest. *Ambio*, *39*, 580–584.
- Matricardi, E. A. T., Skole, D. L., Costa, O. B., Pedlowski, M. A., Samek, J. H., & Miguel, E. P. (2020). Long-term forest degradation surpasses deforestation in the Brazilian Amazon. *Science*, *369*, 1378–1382.
- Mma. (2018). Ministério do meio ambiente. <http://www.mma.gov.br/>. (Accessed 1 August 2017).
- Morandi, P., Marimon-Junior, B., De Oliveira, E., Reis, S., Valadao, M. X., Forsthofer, M., Passos, F., & Marimon, B. (2016). Vegetation succession in the cerrado–amazonian forest transition zone of Mato Grosso state, Brazil. *Edinburgh Journal of Botany*, *73*, 83–93.
- Mueller, B. (2016). Key issues for property rights in Brazil: Implications for the forest code. URL: <http://climatepolicyinitiative.org/publication/key-issues-for-property-rights-in-brazil-implications-for-the-forest-code>.
- Nanni, A. S., Sloan, S., Aude, T. M., Graesser, J., Edwards, D., & Grau, H. R. (2019). The neotropical reforestation hotspots: A biophysical and socioeconomic typology of contemporary forest expansion. *Global Environmental Change*, *54*, 148–159. <https://doi.org/10.1016/j.gloenvcha.2018.12.001>. URL: .
- Nazarova, T., Martin, P., & Giuliani, G. (2020). Monitoring vegetation change in the presence of high cloud cover with Sentinel-2 in a lowland tropical forest region in Brazil. *Remote Sensing*, *12*, 1829. <https://doi.org/10.3390/rs12111829>
- Nepstad, D., McGrath, D., Stickler, C., Alencar, A., Azevedo, A., Swette, B., Bezerra, T., DiGiano, M., Shimada, J., & Seroa da Motta, R. (2014). Slowing Amazon deforestation through public policy and interventions in beef and soy supply chains. *Science*, *344*, 1118–1123. <https://doi.org/10.1126/science.1248525>
- Nicolau, A. P., Flores-Anderson, A., Griffin, R., Herndon, K., & Meyer, F. J. (2021). Assessing SAR C-band data to effectively distinguish modified land uses in a heavily disturbed Amazon forest. *International Journal of Applied Earth Observation and Geoinformation*, *94*, 102214. URL: <https://linkinghub.elsevier.com/retrieve/pii/S0303243420302579>.
- NUGeo. (2018). Núcleo geoambiental - universidade estadual do Maranhão. <http://www.nugeo.uema.br/>.
- Olofsson, P., Foody, G. M., Herold, M., Stehman, S. V., Woodcock, C. E., & Wulder, M. A. (2014). Good practices for estimating area and assessing accuracy of land change. *Remote Sensing of Environment*, *148*, 42–57. <https://doi.org/10.1016/j.rse.2014.02.015>. URL: .
- Pedregosa, F., Varoquaux, G., Gramfort, A., Michel, V., Thirion, B., Grisel, O., Blondel, M., Prettenhofer, P., Weiss, R., Dubourg, V., Vanderplas, J., Passos, A., Cournapeau, D., Brucher, M., Perrot, M., & Duchesnay, E. (2011). Scikit-learn: Machine learning in Python. *Journal of Machine Learning Research*, *12*, 2825–2830.
- Pfaff, A. S. P. (1997). What drives deforestation in the Brazilian Amazon? Evidence from satellite and socioeconomic data. *Policy Research Working Papers*. <https://doi.org/10.1596/1813-9450-1772>
- Pfaff, A. S. (1999). What drives deforestation in the Brazilian Amazon? *Journal of Environmental Economics and Management*, *37*, 26–43. <https://doi.org/10.1006/jeem.1998.1056>
- Pfaff, A., & Robalino, J. (2017). Spillovers from conservation programs. *Annual Review of Resource Economics*, *9*, 299–315.
- Pfaff, A., Robalino, J., Walker, R., Aldrich, S., Caldas, M., Reis, E., Perz, S., Bohrer, C., Arima, E., & Laurance, W. e. a. (2007). Road investments, spatial spillovers and deforestation in the Brazilian Amazon. *Journal of Regional Science*, *47*, 109–123. <https://doi.org/10.1111/j.1467-9787.2007.00502.x>
- Pinto, E., Shin, Y., Cowling, S. A., & Jones, C. D. (2009). Past, present and future vegetation-cloud feedbacks in the Amazon basin. *Climate Dynamics*, *32*, 741–751. <https://doi.org/10.1007/s00382-009-0536-5>. URL: .
- Pontius, R. G. J., & Millones, M. (2011). Death to kappa: Birth of quantity disagreement and allocation disagreement for accuracy assessment. URL: *International Journal of Remote Sensing*, *32*, 4407–4429. <https://doi.org/10.1080/01431161.2011.552923>. arXiv: .
- Project, M. (2021). URL: <https://mapbiomas.org/en>.
- RADAMBRASIL. (1976). *Projeto radambrazil-programa de integração nacional: Levantamento de recursos naturais*. IBGE.
- Rajão, R., Schmitt, J., Nunes, F., & Soares-Filho, B. (2021). *Dicotomia da impunidade do desmatamento ilegal*. Policy Brief.
- Richards, P. (2015). What drives indirect land use change? How Brazil's agriculture sector influences frontier deforestation. *Annals of the Association of American Geographers*, *105*, 1026–1040. <https://doi.org/10.1080/00045608.2015.1060924>
- Richards, P., & VanWey, L. (2015). Where deforestation leads to urbanization: How resource extraction is leading to urban growth in the Brazilian Amazon. *Annals of the*

- Association of American Geographers, 105, 806–823. <https://doi.org/10.1080/00045608.2015.1052337>
- Rochedo, P. R. R., Soares-Filho, B., Schaeffer, R., Viola, E., Szklo, A., Lucena, A. F. P., Koberle, A., Davis, J. L., Rajao, R., & Rathmann, R. (2018). The threat of political bargaining to climate mitigation in Brazil. *Nature Climate Change*, 8, 695–698. <https://doi.org/10.1038/s41558-018-0213-y>
- Setiawan, Y., Yoshino, K., & Prasetyo, L. B. (2014). Characterizing the dynamics change of vegetation cover on tropical forestlands using 250m multi-temporal MODIS EVI. *International Journal of Applied Earth Observation and Geoinformation*, 26, 132–144. <https://doi.org/10.1016/j.jag.2013.06.008>
- Soares-Filho, B. S., Nepstad, D. C., Curran, L. M., Cerqueira, G. C., Garcia, R. A., Ramos, C. A., Voll, E., McDonald, A., Lefebvre, P., & Schlesinger, P. (2006). Modelling conservation in the amazon basin. *Nature*, 440, 520–523.
- Souza, A., Monteiro, A. M. V., Rennó, C. D., Almeida, C. A., Valeriano, D. d. M., Morelli, F., Vinhas, L., Maurano, L. E. P., Adami, M., Escada, M. I. S., et al. (2019). *Metodologia utilizada nos projetos prodes e deter*. Brazil: INPE: São José dos Campos.
- Souza, C. M., Shimbo, J. Z., Rosa, M. R., Parente, L. L., Alencar, A., Rudorff, B. F. T., Hasenack, H., Matsumoto, M., Ferreira, L., Souza-Filho, P. W. M., de Oliveira, S. W., Rocha, W. F., Fonseca, A. V., Marques, C. B., Diniz, C. G., Costa, D., Monteiro, D., Rosa, E. R., Véllez-Martin, E., ... Azevedo, T. (2020). Reconstructing three decades of land use and land cover changes in brazilian biomes with landsat archive and earth engine. *Remote Sensing*, 12. <https://doi.org/10.3390/rs12172735>. URL: <http://www.mdpi.com/2072-4292/12/17/2735>.
- Stehman, S. V. (2014). Estimating area and map accuracy for stratified random sampling when the strata are different from the map classes. *International Journal of Remote Sensing*, 35, 4923–4939. <https://doi.org/10.1080/01431161.2014.930207>. URL: .
- Sulla-Menashe, D., & Friedl, M. (2018). User guide to collection 6 MODIS land cover (MCD12Q1 and MCD12C1) product. NASA EOSDIS land processes DAAC. URL: https://lpdaac.usgs.gov/sites/default/files/public/product_documentation/mcd12_us_er_guide_v6.pdf.
- Valente, R. (2021). Reportagem: Rubens Valente - O monitoramento do Cerrado está à beira do colapso por falta de dinheiro. URL: <https://noticias.uol.com.br/colunas/rubens-valente/2021/09/20/cerrado-programa-verbas-monitoramento-cancelamen-to.htm>.
- Wang, J., Chagnon, F. J. F., Williams, E. R., Betts, A. K., Renno, N. O., Machado, L. A. T., Bisht, G., Knox, R., & Bras, R. L. (2009). Impact of deforestation in the Amazon basin on cloud climatology. URL: *Proceedings of the National Academy of Sciences*, 106, 3670–3674. <https://doi.org/10.1073/pnas.0810156106>. arXiv:[http://www.pnas.org/content/106/10/3670](http://www.pnas.org/content/106/10/3670.full.pdf).
- West, T. A., & Fearnside, P. M. (2021). Brazil's conservation reform and the reduction of deforestation in amazonia. *Land Use Policy*, 100, 105072. <https://doi.org/10.1016/j.landusepol.2020.105072>. URL: .
- Zi, Y., Xie, F., & Jiang, Z. (2018). A cloud detection method for landsat 8 images based on pancanet. *Remote Sensing*, 10, 877. <https://doi.org/10.3390/rs10060877>. URL: <http://www.mdpi.com/2072-4292/10/6/877>.